Journal of Computer-Aided Molecular Design, **16:** 635–651, 2002.
KLUWER/ESCOM

Parametrization of a force field for metals complexed to biomacromolecules: applications to Fe(II), Cu(II) and Pb(II)

Laurent David[1,*,†], Patricia Amara[2], Martin J. Field[2] & François Major[1]
[1]*Département d'Informatique et de Recherche Opérationnelle, Université de Montréal, C.P. 6128, Succ. Centre-Ville, Montréal, Québec, Canada H3C 3J7,* [2]*Laboratoire de Dynamique Moléculaire, Institut de Biologie Structurale – Jean-Pierre Ebel, 41 Rue Jules Horowitz, F-38027 Grenoble Cedex 01, France*

Received 28 January 2002; accepted in final form 24 October 2002

Key words: metals, lead, force fields, parametrization, crystallographic data

Summary

Although techniques for the simulation of biomolecules, such as proteins and RNAs, have greatly advanced in the last decade, modeling complexes of biomolecules with metal ions remains problematic. Precise calculations can be done with quantum mechanical methods but these are prohibitive for systems the size of macromolecules. More qualitative modeling can be done with molecular mechanical potentials but the parametrization of force fields for metals is often difficult, particularly if the bonding between the metal and the groups in its coordination shell has significant covalent character. In this paper we present a method for deriving bond and bond-angle parameters for metal complexes from experimental bond and bond-angle distributions obtained from the Cambridge Structural Database. In conjunction with this method, we also introduce a non-standard energy term of gaussian form that allows us to obtain a stable description of the coordination about a metal center during a simulation. The method was evaluated on Fe(II)-porphyrin complexes, on simple Cu(II) ion complexes and a number of complexes of the Pb(II) ion.

Introduction

Two of us (LD and FM) have been interested in investigating the structure and the lead-binding sites of autolytic RNA fragments (David et al., 2001) using molecular dynamics simulations in conjunction with an empirical force field description of the system's potential energy surface. Unfortunately, however, few, if any, parameters for the Pb(II) ion appear to exist in the literature, at least for the force fields, such as AMBER (Cornell et al., 1996) and CHARMM (Brooks et al., 1983), that are commonly used for simulations of proteins and nucleic acids. Indeed, the parametrization of force fields for metals poses problems that do not exist when parametrizing force fields for organic molecules consisting solely of first and second row atoms. This is because metals show a very wide range of bonding behavior – for example, the bonding can range between purely covalent to purely ionic and they can have variable coordination geometries, sometimes with little difference in energy between them. In addition, metals are often highly charged, making effects such as polarization important, and they can exist in different spin states. As a result, force field development for metals remains an open problem although considerable work has been done in this area (for reviews see Hay, 1993, Zimmer, 1995 and the articles in Coord. Chem. Rev. 212, 2001). Some examples of the parametrization of force fields for specific metals include work on molybdenum in *tripod*-$Mo(CO)_3$ compounds (Hunger and Huttner, 1998; Hunger et al., 1998) and on the alkali metals, Li^+, Na^+ and K^+, in interaction with carbonyl oxygens (Roux and Karplus, 1995).

In this paper, we describe the parametrization of a force field for the Pb(II) ion interacting with RNA that can be used in conjunction with the CHARMM 27 all-atom force field for nucleic acids (Foloppe and

*Present address : AstraZeneca R&D Lund, Sweden.
†To whom correspondence should be addressed.
E-mail: Laurent.David@astrazeneca.com

Mackerell, 2000). The fact that the coordination sites and, hence, the coordinating ligands of the Pb(II) ion in our system (leadzyme) are uncertain makes this more complicated than for the cases where the ligands are known. In the latter instances, it would be possible to select examples of complexes with the appropriate coordination pattern and then use their structures and other properties, obtained either from experiment or from high-level *ab initio* quantum mechanical (QM) calculations, as observables against which to parametrize the force field. In the leadzyme case, this would mean having to identify all possible coordination patterns and parametrizing each of them separately.

Instead, we have preferred to start with an approximate approach which can be used to generate parameters for the short-range energy terms in a force field, the bonds and bond angles, that determine the coordination pattern of a metal ion in different environments. We have done this by interrogating the Cambridge Structural Database (CSD) (Allen et al., 1991) for structures containing the appropriate metal ion, analyzing the structures to obtain statistical distributions of bond distances and bond angles and then using this data to derive appropriate force field parameters. We have applied this method to the Pb(II) ion but we also describe results for the Cu(II) and Fe(II) ions which we took as test cases to validate the scheme. We initially derived parameters for harmonic bond and bond-angle energy terms but we found that these were not sufficiently flexible to describe the variable coordination states for the Pb(II) ion and so we have developed an energy term of an alternative form. Although the statistical method can give bond and bond-angle parameters, these have to be supplemented with parameters for the other terms in the force field, such as the electrostatic and Lennard-Jones energies. These we obtained in a more traditional way by employing a model set of Pb(II) complexes chosen from the CSD.

The outline of this article is as follows. The protocol used to obtain bond and bond-angle parameters from crystallographic data and the general parametrization strategy for the Pb(II) ion are described in section 2. Section 3 discusses and analyzes the results of our statistical approach to obtaining bond and bond-angle parameters for the Pb(II) force fields and section 4 concludes.

Methods

Calculation of bond and bond-angle parameters

Consider a harmonic bond energy term between atoms of two different types, t_1 and t_2. The energy will be $K_b(d - d_0)^2$ where d is the distance between the two atoms and K_b and d_0 are the force constant and the equilibrium bond distance for the term, respectively. If the potential energy function for the system consists solely of this term, the distribution of bond distances in the canonical ensemble will have the Boltzmann form. Thus, we can compute the probability of finding a bond distance d between $x - \delta$ and $x + \delta$ as:

$$\begin{aligned} \mathcal{P}_{x-\delta}^{x+\delta} &\propto \int_{x-\delta}^{x+\delta} \mathrm{d}u \exp\left[-\frac{K_b}{RT}(u - d_0)^2\right] \\ &\propto \operatorname{erf}\left[\sqrt{\frac{K_b}{RT}}(x - d_0 + \delta)\right] \\ &\quad - \operatorname{erf}\left[\sqrt{\frac{K_b}{RT}}(x - d_0 - \delta)\right] \end{aligned} \tag{1}$$

where R is the gas constant and T is the temperature. Taking the logarithm of the distribution and expanding in powers of $x - d_0$ gives the following expression for a potential of mean force (PMF):

$$\begin{aligned} \ln \mathcal{P}_{x-\delta}^{x+\delta} &= \ln\left(\operatorname{erf}\left[\sqrt{\frac{K_b}{RT}}\delta\right]\right) + f(\delta)(x - d_0)^2 \\ &\quad + O\left((x - d_0)^4\right) \end{aligned} \tag{2}$$

where $f(\delta)$ is a function of $\sqrt{K_b/RT}$ and of δ and whose form need not concern us here.

Equation 2 is an approximate expression for the logarithm of the probability distribution function of bond lengths. Suppose now that we have an experimental set of distances between atoms of type t_1 and t_2 and from which we can derive an experimental distribution by binning the values using a step equal to 2δ and normalizing. We then make the assumption that the logarithm of the probability distribution of equation 2 can be fitted to a quadratic of the form:

$$ax^2 + bx + c = a\left(x + \frac{b}{2a}\right)^2 + c - \frac{b^2}{4a} \tag{3}$$

Comparing equations 2 and 3 gives expressions for the force constant and the equilibrium distance:

$$K_b = \frac{RT}{\delta^2}\left(\operatorname{erf}^{-1}\left[\exp\left(c - \frac{b^2}{4a}\right)\right]\right)^2 \tag{4}$$

$$d_0 = -\frac{b}{2a} \tag{5}$$

where erf^{-1} is the inverse error function.

A number of approximations have been made in the above scheme. The principal one is that the validity of equation 1 assumes that the degree of freedom being considered is independent of the other variables in the system. This will not, of course, be true in general because, in a molecule of any complexity, the various terms in the energy function are highly coupled. However, as will be seen below, this assumption is probably a reasonable first approximation for bonds and bond angles because their energies are determined primarily by their associated (and neighboring) bond and bond-angle force field terms and not by interactions with atoms that are further away. The bond-angle energy term can be treated in a similar way to the bond term as it too is harmonic with the form $K_\theta(\theta-\theta_0)^2$ where θ is the bond angle and K_θ and θ_0 are the force constant and the equilibrium value for the angle, respectively.

We have used the above formulae, equations 4 and 5, to determine parameters for bond and bond-angle force field terms for the Cu(II), Fe(II) and Pb(II) ions. The experimental bond and bond-angle distributions were calculated using data extracted from the CSD. In our use of data from the CSD, we implicitly assume that the crystal environment does not play a major role in determining the values of the bond and bond angles that were observed. We also took all the structures that were available for a given metal ion, independent of the temperature at which they had been obtained, because there were insufficient to consider only a subset solved within a given temperature range. In principal the structures will change with temperature but in many cases these variations will be small. Thus, for example, Byrn and Strouse have shown that different temperatures do not alter significantly the Fe–N bond distance in Fe(III)–porphyrins (Byrn and Strouse, 1991).

As an alternative to the scheme outlined above, we tried a second approach to determine bond parameters. This involves taking the data from the CSD to generate a radial distribution function $g_{ab}(r)$ for pairs of atoms and using this to determine the potential of mean force between the atoms from the equation:

$$\mathcal{W}_{ab}(r) = -RT \ln\left[g_{ab}(r)\right] \tag{6}$$

This PMF can then be fitted to a harmonic expression of the same form as equation 3 from which the bond parameters can be determined as before. This method is derived from the one developed for pair potentials by Sippl et al. (Sippl et al., 1986). To terminate this section, we note that in what follows we refer to the PMFs coming from equations 2 and 6 as the 'CSD' and 'Sippl' PMFs, respectively.

An alternative potential energy term for metal ions

In this section we propose a novel potential energy term (denoted, henceforth, for convenience as NPE) for metal ions that is more suited than the conventional harmonic form for the description of the range of coordination states that we observed for Pb(II) in structures from the CSD. As in the previous section, we take the probability distributions for bond distances and bond angles and, from these, we compute PMFs as a function of the distances and angles. Thus, the PMF, $\mathcal{W}(x)$, for a variable x with distribution $\mathcal{P}(x)$ is:

$$\mathcal{W}(x) = -RT \ln\left[\mathcal{P}(x)\right] + c' \tag{7}$$

where c' is an arbitrary constant. It is to be noted that we took T to be constant with a value of 297 K which is the highest temperature at which any of the structures had been determined.

Again, as in the previous section, we assume that the bond and bond-angle variables are independent of each other and so we can write the total energy of the system as a sum of PMF-like terms for each bond and bond-angle variable. The problem then is to fit the observed PMFs so that they can be used in the calculation of the energy. Inspection of the bond and bond angle distributions for Pb(II) showed that a set of, at most, three Gaussians were appropriate and so we chose the form:

$$\mathcal{P}(x) = \sum_{i=1}^{3} a_i \exp\left(-b_i(x - c_i)^2\right) \tag{8}$$

where a_i is a scale parameter, b_i is a force constant and c_i is an equilibrium value for the parameter x. Note that the temperature in equation 8 was taken to be room temperature, as in equation 7. The parameters a_i and b_i were optimized by minimizing the differences between the energy coming from the calculated and observed distributions whereas the c_i were set to the most important minima deduced from the observed distribution. The fit was performed with a downhill simplex simulated annealing method (Press et al., 1996).

Pb(II) ion parameter refinement

A final force field for the Pb(II) ion contains not only bond and bond-angle terms but also terms for proper and improper dihedral angles and for electrostatic and Lennard-Jones interactions. In preliminary

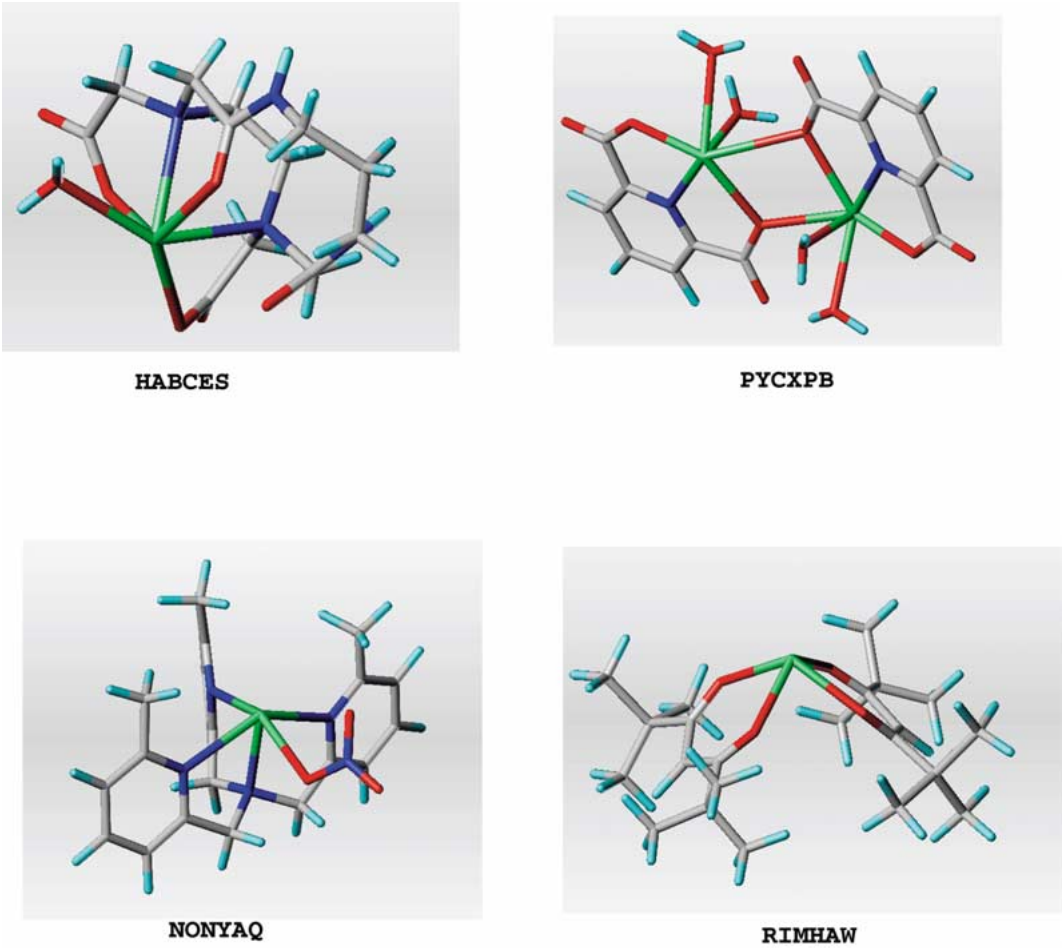

Figure 1. The structures of the Pb(II) ion complexes of the training set taken from the CSD. Atom colors: Pb is in green, O in red, N in blue, C in gray and H in cyan.

investigations, we found that the inclusion of proper-dihedral-angle energy terms made little difference to the final results and so we decided to exclude them.

For the parametrization of the remaining non-bonding energy terms, we employed a set of four Pb(II) ion complexes taken from the CSD as the training set. The complexes were HABCES (Inoue et al., 1993), PYCXPB (Beveridge and Bushnell, 1979), NONYAQ (Zhihui et al., 1997) and RIMHAW (Krisyuk et al., 1997) and their structures are shown in Figure 1. We then geometry optimized these complexes with a high-level *ab initio* QM method. The geometry-optimized structures were taken as our reference structures and, as they were performed in vacuum, the minimizations helped to remove any strain due to the crystal environment. The QM calculations were performed with the Jaguar program using density functional theory (DFT) with the B3-LYP functional (Jaguar, 2000). The basis set was the all-electron 6-311G set for the organic atoms and the valence-electron/effective-core-potential set LACV3P for lead. We also did calculations for the complex PYCXPB with a larger lead basis set (LACV3P^{**++}) to check if there were any significant differences in results but we found none. The atomic charges for the force fields of each of the optimized complexes were obtained with the electrostatic potential fitting method in Jaguar (Woods et al., 1990) which not only reproduces the total charge on the complex but also the dipole moment. These charges were used for all models including both Lennard-Jones (LJ) models ('LJ1' and 'LJ2') that are described later on.

The optimization of the LJ parameters was done alone and also together with a refinement of the bond

and bond-angle parameters obtained by the method of section 2.1. This was done to see what effect consideration of specific complexes would have on the values of the general bond and bond-angle parameters obtained from the statistical procedure. To perform the parameter optimization, the *ab initio* structures served as our reference structures. For each complex we constructed an MM model and then we optimized the Pb(II) bond, bond-angle and LJ parameters so that the RMS coordinate deviations between the *ab initio* structures and the MM structures were minimized. The parameter optimization was first performed with the downhill simplex simulated annealing method (Press et al., 1996), but eventually a genetic algorithm (Dorsey et al., 1994) was preferred because convergence was more effective. MM energy minimizations were necessary at each step of the parameter optimization procedure and were performed with the fast and efficient truncated-Newton method (Derreumaux et al., 1994). Convergence was considered attained when the RMS gradient was smaller than 10^{-3} kcal mol^{-1} Å^{-1} or was stopped when more than 2000 steps had been carried out. First and second derivatives were computed analytically for all energy terms. All calculations were performed on Linux/Pentium II 650 Mhz or SGI R10000 computers, in serial for the simplex optimizations and in parallel, on a Linux 10-node cluster, for the genetic algorithm calculations.

Results and analysis

Obtaining bond and bond angle parameters from structural data

Validation of the method

We began by testing the bond and bond-angle parameter-fitting procedure described in section 2.1 using theoretical bond distance and bond-angle distributions obtained from a stochastic molecular dynamics (MD) simulation of the leadzyme (without the lead). The simulation was performed for 1 ns starting from the leadzyme NMR structure (Hoogstraten et al., 1998) (Protein Data Bank (Bernstein et al., 1977) code 1ldz), using the program UHBD (Davis et al., 1991) and the CHARMM 27 all-atom force field (Foloppe and Mackerell, 2000). The temperature of the simulation was 300 K, the integration time-step was 1 fs and the friction coefficient for each atom was 10 s^{-1}. Counterions were added to neutralize the system (23 Na^+ and 3 Mg^{2+}) and the solvent was represented by the Generalized-Born (GB) implicit solvation model (Qiu et al., 1997). The forces due to the solvent were updated every 5 fs, the effective radii every 10 fs and the GB non-bonding interaction list every 10 fs with a 20 Å cutoff (David et al., 2000). Structures were saved every 500 fs during the simulation giving 2000 structures in all for analysis.

We computed the bond and bond-angle parameters associated with the backbone phosphorus atoms using both methods described in section 2.1 and compared them with the parameters actually used in the simulation. The CHARMM atom types (with PDB names in brackets) of the atoms involved are P (P), ON3 (O1P,O2P), ON2 (O3′,O5′) and CN8 (C5′). Comparisons of the bond and bond-angle parameters are given in Tables Ia and Ib, respectively.

Table Ia shows that the equilibrium bond distances are very well reproduced except for the pair C5′–O5′ where the difference is about 0.03 Å. This variation can be explained as being due to a strain between the hydrogens bonded to C5′ and the atom O5′ which forces the elongation of the bond. The force constants are also well-reproduced when the equilibrium distances are used for the parameter determination, except for the P–O1P value which is underestimated by about 10%. When the 'Sippl' PMF method of equation 6 is employed, however, the force constants are all underestimated with the largest deviation being about 15%. This discrepancy was also observed for bond-angle parametrization (results not shown) and so we decided to continue with the 'CSD'-PMF method of equation 3 uniquely. The equilibrium bond angles from Table Ib are, like the equilibrium bond distances, close to their CHARMM values. The average deviation is about 2° except for the angle C5′–O′–P where a shift of about 14° is observed. This is mainly due to non-bonding contacts between the phosphorus and the hydrogens bound to C5′. The bond-angle force constants are also reasonably well-reproduced with all but one being underestimated. The largest deviations, of about 20%, occur for the angles O3′–P–O5′ and O5′–P–O1P.

The above results indicate that the statistical method is capable of producing reasonable bond and bond angle parameters. The errors for most of the equilibrium bond distances and bond angles are within an acceptable range which, following Hancock, can be defined as about 0.01 Å for a bond distance and about 2° for a bond angle (Hancock, 1989). It is to be noted that the statistical method, as expected, does

Table Ia. Computed bond parameters for both methods ('CSD' and 'Sippl' PMF) described in section 2.1, compared with the ones from the CHARMM 27 all-atom force field (Foloppe and Mackerell, 2000). The CHARMM atom types are listed for the atoms along with the PDB names in brackets if these are different. Distances are in Å, force constants are in kcal mol^{-1} $Å^{-2}$.

Atom Type		'CSD' PMF		'Sippl' PMF		CHARMM Values	
# 1	# 2	K_b	d_0	K_b	d_0	K_b	d_0
P	ON2(O1P)	525	1.48	485	1.48	580	1.48
P	ON2(O2P)	586	1.48	512	1.49	580	1.48
P	ON3(O3′)	271	1.60	250	1.60	270	1.60
P	ON3(O5′)	289	1.60	248	1.60	270	1.60
CN8(C5')	ON3(O5′)	343	1.45	315	1.46	340	1.43

Table Ib. Computed bond angle parameters for the 'CSD' PMF method, described in section 2.1, compared with the ones from the CHARMM 27 all-atom force field. The PDB names are used to identify the atoms. Angles are in degrees, force constants are in kcal mol^{-1} rad^{-2}.

Atom Type			'CSD' PMF		CHARMM Values	
# 1	# 2	# 3	K_θ	θ_0	K_θ	θ_0
O3′	P	O5′	64.0	103.9	80.0	104.3
O3′	P	O1P	98.0	109.4	98.9	111.6
O3′	P	O2P	86.0	109.6	98.9	111.6
O5′	P	O1P	77.0	109.1	98.9	111.6
O5′	P	O2P	93.0	109.6	98.9	111.6
O1P	P	O2P	123.0	116.8	120.0	120.0
C5′	O5′	P	24.0	133.7	20.0	120.0

not work well for dihedral-angle parameters because of the coupling of this energy term to the other bonding and non-bonding energy terms of the surrounding atoms (results not shown).

Fe(II) bond and bond-angle parameters

Due to its presence in heme-containing proteins, several force fields contain parameters for the Fe(II) ion and, as such, it is an appropriate ion upon which to test our parametrization procedure. We selected from the CSD all structures involving Fe(II) and having a coordination with the moieties pyrrole and imidazole.

In the CSD, the nitrogen coordinating the Fe(II) in all our selected complexes had the same type, N.2, which corresponds to an sp2 nitrogen atom. All Fe–N.2 distances were computed for each complex, giving 433 unique distances in all, and these were binned using a width of 0.02 Å for the imidazole and 0.01 Å for the pyrrole (depending on the size of the distribution) to give the probability distribution for distances as a function of bond length. Extreme values at the edges of the distribution were removed. The final distributions for the imidazole and pyrrole nitrogen are displayed in Figures 2(a) and 2(b), respectively. Inspection of the pyrrole distribution shows that there are two distinct distributions with peaks at distances of about 1.98 and 2.09 Å, respectively. We term distances in these two peaks, class 1 and class 2, respectively. The distance distribution obtained with the imidazole moiety shows also two distinct peaks at distances of about 2.03 and 2.18 Å, respectively.

The presence of distinct peaks in the distribution indicates that different atom types have to be used for the parametrization of the bond distances in each peak, in contrast to the notation in the CSD where all the nitrogen atoms are of the same type (N.2). In the CHARMM force field (Mackerell et al., 1988) there are two nitrogen atom types, one for the pyrrole (CHARMM type NPH) and one for imidazole (CHARMM type NR2). In the QUANTA ver-

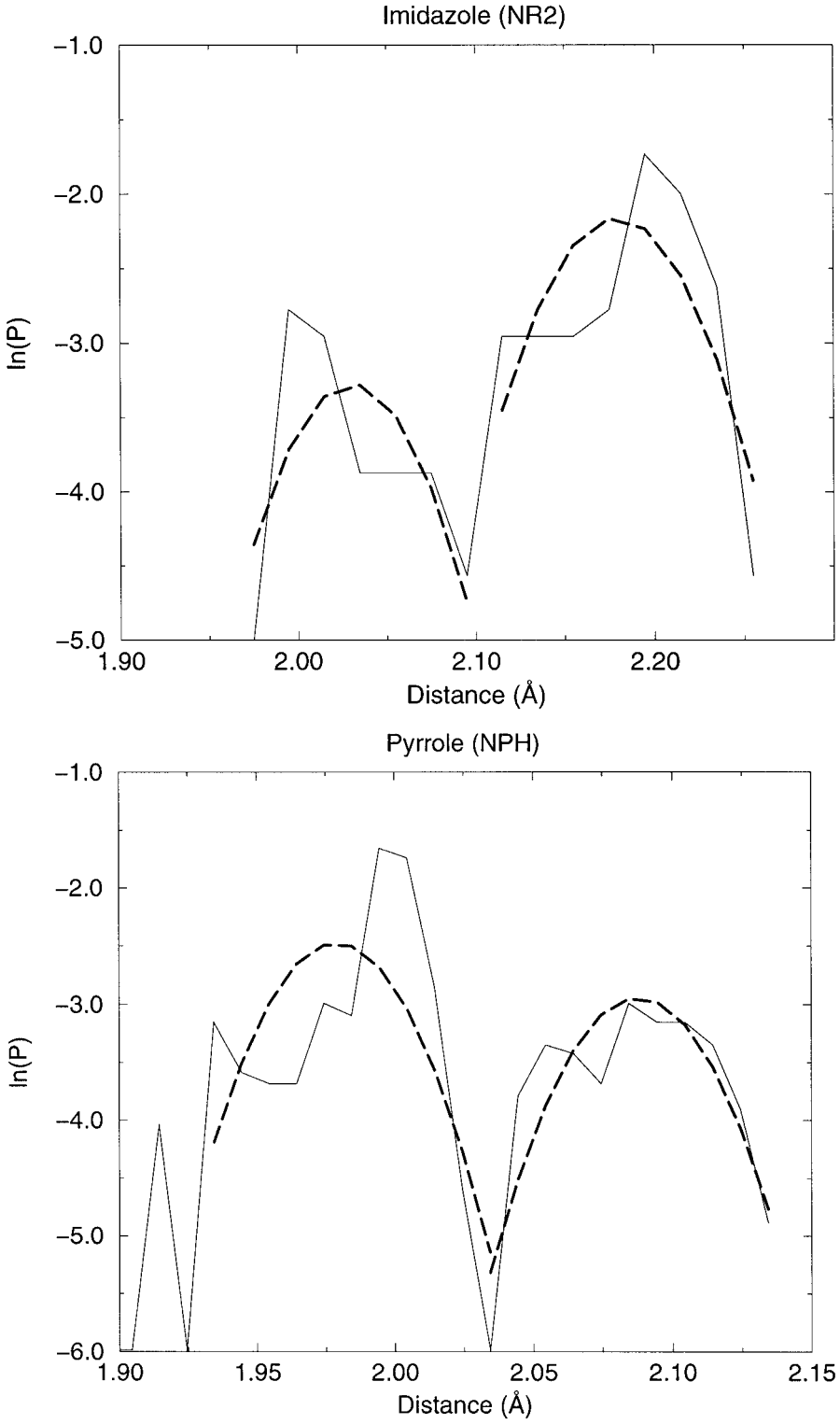

Figure 2. (a) Logarithm of the Fe(II)–N.2-Fe distance distribution obtained from the imidazole CSD structures as a function of distance. The dot-dashed lines are the quadratic fits.
(b) Logarithm of the Fe(II)–N.2-Fe distance distribution obtained from the pyrrole CSD structures as a function of distance. The dot-dashed lines are the quadratic fits.

Table IIa. 'CSD' PMF and existing bond parameters for nitrogen–Fe(II) bonds. NPH is a pyrrole nitrogen atom; NPH* is a pyrrole nitrogen atom with the Fe outside of the porphyrin plane; NR2 is a imidazole nitrogen atom; N5R is a nitrogen in a five membered aromatic ring. The class column represents the class of bond distances used in the parametrization (see Figure 2). IS, HS and LS stand for intermediate, high and low spin, respectively. Distances are in Å, force constants are in kcal mol^{-1} $Å^{-2}$.

Atom Bound to Fe(II)			Parameter		
Force Field	Nitrogen Type	Occurrence	Class	K_b	d_0
'CSD PMF'	NR2.1	18	1	283	2.04
	NR2.2	59	2	66	2.18
	NPH	261	1	361	1.98
	NPH*	128	2	521	2.09
CHARMM (Mackerell et al., 1998)	NPH			270	1.96
	NR2			65	2.20
QUANTA (Quanta,)	N5R			65	1.98
MM2(Munro et al., 1992)	NPH(IS)			345	1.96
	NPH(HS)			385	2.09
	NPH(LS)			385	1.99

Table IIb. Statistical and existing bond angle parameters for bond angles involving nitrogen and Fe(II) ions. The nitrogen atom types are explained in the caption to Table IIa. The carbon types are: C.1 and C.2 – CSD atom types for sp and sp2 hybridized carbons, respectively; CM – CHARMM atom type for the carbon in carbon monoxide; CPH1 – CHARMM atom type for the carbon in imidazole linked to another carbon; CPH2 – CHARMM atom type for the carbon in imidazole linked to two nitrogens; CPA – CHARMM atom type for the carbon in heme α carbon. Angles are in degrees, force constants are in kcal mol^{-1} rad^{-2}.

Force Field	# 1	# 2	# 3	Occurrence	K_θ	θ_0
'CSD PMF'	C.2	N.2(NPH)	Fe	738	135	126.7
	C.2	N.2(NR2)	Fe	87	89	127.7
	C.2	N.2(NR2)	Fe	35	32	112.9
	N.2(NPH)	Fe	N.2(NPH)	294	42	90.1
	C.1	Fe	N.2(NPH)	32	213	90.7
CHARMM (Mackerell et al., 1998)	CPA	NPH	Fe		96	128.1
	CPH1	NR2	Fe		30	133.0
	CPH2	NR2	Fe		30	123.0
	NPH	Fe	NPH		14	90.0
	CM	Fe	NPH		50	90.0

sion of the CHARMM force field (Mackerell et al., 1998) there is only a single nitrogen that interacts with Fe(II) (QUANTA type N5R). Parameters for the Fe(II)-pyrrole interaction, derived by Munro et al. for the MM2 force field also exist (Munro et al., 1992; Allinger, 1977) but these vary depending upon the spin state of the iron to which the nitrogen is bound. All parameters for bonds and bond angles are given in Tables IIa and IIb respectively.

In our calculations we settled on four atom types after analysis of the distance data. These were NPH, NPH* and NR2.1, NR2.2 which correspond to two pyrrole atom types and two imidazole atom types, respectively. The difference between the two pyrrole types is that NPH represents the case where the Fe(II) has either no or two axial ligands and NPH* the case where there is a single ligand. Most (89%) of the pyrrole nitrogen–Fe(II) distances of class 1 involve atom type NPH (i.e. symmetric axial linking) whereas most (65%) of the pyrrole nitrogen–Fe(II) distances of class 2 involve NPH* and, as a result of the asymmetric ligand conformation, the Fe(II) ion is pushed out of the

Table III. 'CSD' PMF and MOMEC bond parameters for atoms interacting with Cu(II). The N.2 parameters were obtained with the following structures: [a]imidazole; [b]benzimidazole; [c]pyrazole; [d]all structures. The MOMEC results are from references Bernhardt and Comba, 1992 (N.imine, N.amine and OC (carboxylic oxygen)) and Bol et al., 1998 (NAH). NAH is an atom type for imidazole nitrogen (i.e. N.imine specific for imidazole). Distances are in Å, force constants are in kcal mol^{-1} $Å^{-2}$.

Force Field	Atom	Occurrence	K_b	d_0
'CSD' PMF	N.2[a]	701	138.4	1.99
	N.2[b]	358	167.7	1.99
	N.2[c]	194	285.7	1.98
	N.2[d]	1253	178.8	1.99
	N.3	213	95.4	2.05
	O.co2	112	440.0	1.95
MOMEC	N.imine		172.0	1.94
	N.amine		172.0	1.97
	NAH		257.0	1.98
	OC		228.0	1.90

plane of the prosthetic group. Only 16% of in-plane pyrrole nitrogens have a Fe(II) distance larger than 2.05 Å, whereas 67% of out-of-plane pyrrole nitrogens have a Fe(II) distance larger than 2.05 Å.

Available bond parameters from CHARMM, QUANTA and MM2 differ for both nitrogen types NR2 and NPH. Our subtype NR2.2 corresponds well with the atom type NR2 from CHARMM as it has a very similar equilibrium distance and force constant. In contrast, the subtype NR2.1 differs substantially from the CHARMM and QUANTA imidazole types. Our computed NPH atom-type parameters are in reasonable agreement with the CHARMM NPH values and very similar to those of the MM2 NPH(IS) type. The force constants in all cases are larger than 250 kcal mol^{-1} $Å^{-2}$, and the equilibrium distances differ by 0.022 Å and 0.025 Å from the CHARMM and MM2 values, respectively. Our atom type NPH* has similar parameters to MM2 NPH(HS) with a larger force constant but a very similar equilibrium distance, 2.09 Å versus 2.085 Å (see Table IIa).

Computed bond-angle parameters are compared with the CHARMM parameters in Table IIb. Our parameters for the angle term C.2-NPH-Fe are in reasonable agreement to the CHARMM values for the angle term CPA-NPH-Fe. For bond angles with a central imidazole nitrogen, both CHARMM and our results show two terms. In one of our terms C.2-NR2-Fe, the equilibrium angle of 112.9° differs from the equivalent CHARMM value for CPH2-NR2-Fe by about 10° although both force constants are very similar. For the second terms, C.2-NR2-Fe and CPH1-NR2-Fe, the equilibrium distances are in good agreement but our force constant is three times larger. The other two angle terms listed in the table with Fe as the central atom show similar behaviors. The equilibrium distances are in good agreement but the force constants are larger by a factor of three to four than the CHARMM values.

Cu(II) bond parameters

Comba et al. have performed work that permits the MOMEC force field to describe transition metal complexes (Bernhardt and Comba, 1992; Comba et al., 1995; Bol et al., 1998). Although they use a potential energy function with a form different from that of the CHARMM force field, we still thought it valuable to check our method against their data for the case of the Cu(II) ion. The structures of four classes of complex were taken from the CSD – those with oxalate, pyrazole, imidazole and benzimidazole ligands – and the bond parameters between the Cu(II) ion and the carboxylic oxygen of oxalate and the nitrogens of the remaining ligands were computed. The results are shown in Table III along with the values from the MOMEC force field.

In our calculations, the CSD atom types N.2 and N.3 are used for sp2 and sp3 nitrogen, respectively, and O.co2 for carboxylic oxygen. For the N.2 atom type, we derived four sets of parameters – three sets using distances from each N.2-containing ligand separately and one set using the pooled set of N.2–Cu(II) ion distances. The equilibrium bond distances for all sets of N.2-atom-type parameters are in good agreement whereas the force constants vary within the range 140–280 kcal mol^{-1} $Å^{-2}$. The average parameters, however, resemble closely those for the N.imine atom type from the MOMEC force field. The results are similar for the N.3 and O.co2 atom types with equilibrium values in close agreement and force constants showing more variation.

Parametrizing a Pb(II) ion force field

The results of section 3.1 showed that deriving reasonable bond and bond angle parameters from statistical analysis of structural data is possible and so we decided to follow the same strategy for the parametrization of a force field for the Pb(II) ion for future work on the leadzyme. In our search of the CSD, we retained structures that contained Pb(II) ion–other

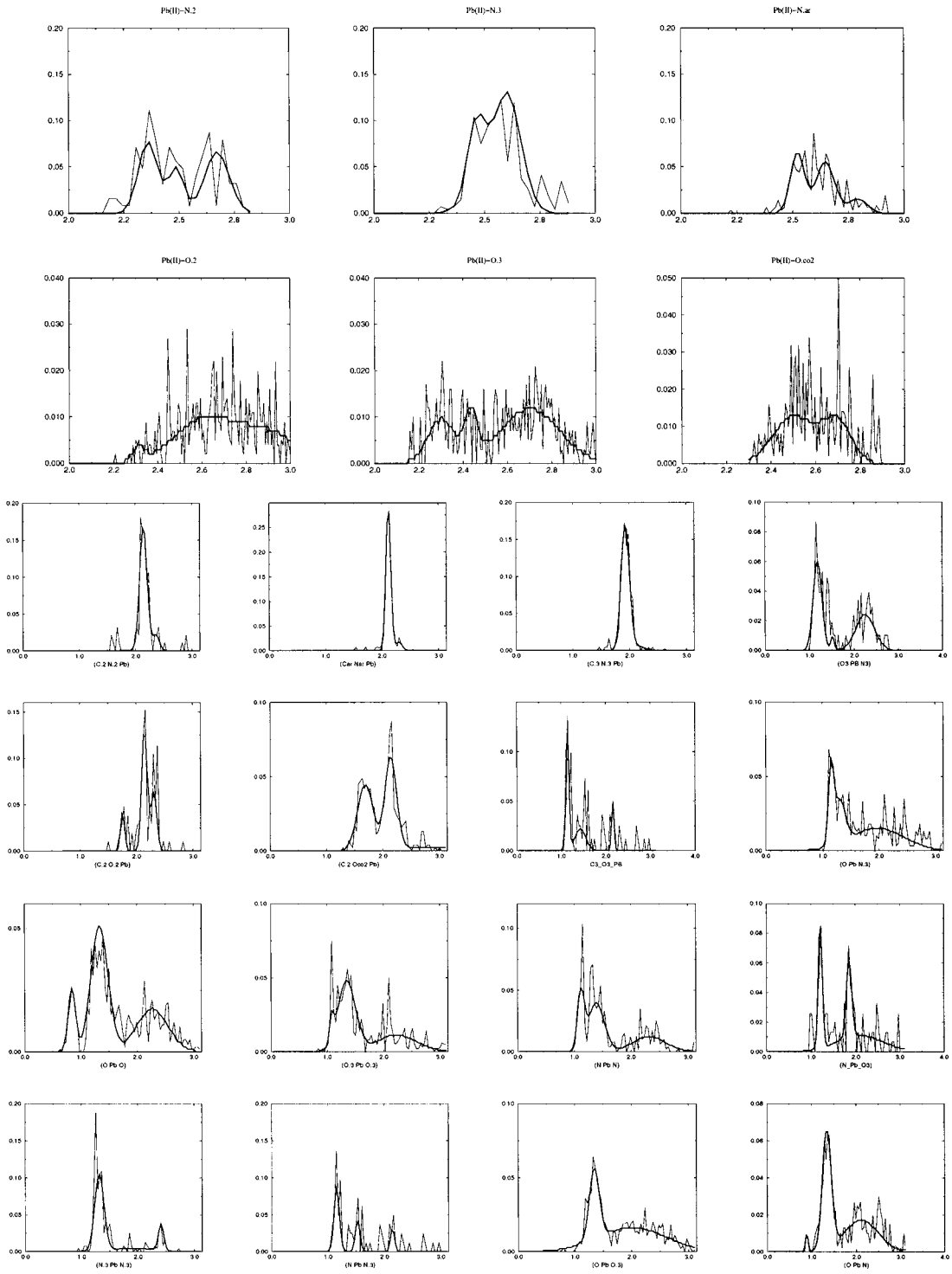

Figure 3. (a) Distance distributions obtained for Pb(II) complexes from CSD data with superimposed Gaussian fits. The x-axes are the distance (Å) and the y-axes are their probabilities.
(b) Angle distributions obtained for Pb(II) complexes from CSD data with superimposed Gaussian fits. Type N stands for N.2 and N.ar and type O for O.2 and O.co2. The x-axes are the angles (in radians) and the y-axes are their probabilities.

Table IV. Details of the interactions between Pb(II) and other atoms in the structures extracted from the CSD. Distances are in Å.

Atom Name	Atom Type	Distance to Pb	Standard Deviation	Occurrence
O.co2	Oxygen in carboxylate or phosphate	2.55	0.17	504
O.2	Oxygen sp2	2.68	0.25	255
O.3	Oxygen sp3	2.61	0.23	1327
N.2	Nitrogen sp2	2.55	0.18	232
N.ar	Aromatic nitrogen	2.62	0.12	259
N.3	Nitrogen sp3	2.57	0.16	265
C.ar	Aromatic carbon	2.50	0.32	148

atom interactions that are likely to be similar to those found in the leadzyme RNA. Due to the paucity of data, we used all structures containing at least one Pb(II) ion and having interactions to the types of atoms that we were interested in, although we excluded interactions with distances of more than 2.9 Å from our analysis. The atoms involved in the interactions are listed in Table IV along with their CSD designation, the frequencies of occurrence of the interactions and the interaction mean lengths and standard deviations. We chose to use CSD atom types for the non-metal atoms in the interactions so as to restrict the number of types that we needed to consider. In addition, for the angle parameters, we tried to treat all sp2-hybridized nitrogens and all oxygens as single types to see if the number of parameters we needed to derive could be reduced even further. It is clear from Table IV that the bond lengths between Pb(II) and the other atoms have means that are significantly larger than those involving Fe(II) or Cu(II). Taking Pb(II)–nitrogen interactions as an example, we find that the sum of the Pb(II) and nitrogen covalent radii (1.47 and 0.75 Å, respectively (Winter, 2001)) is about 0.4 Å less than the average distance for these interactions found in Table IV, which implies that most Pb(II)–ligand bonds have a weak covalent character (Harrison, 1976). This weak character for the interactions is also indicated by the broad bond-length distributions which results in low values for the bond-term force constants.

The bond and bond-angle distributions obtained for Pb(II) from the CSD are shown in Figures 3(a) and 3(b), respectively. Also plotted are the fits of the distributions to the sum of Gaussians expression of equation 8. The bond and bond angle parameters resulting using the CSD data are given in Tables Va and

Table Va. Statistical bond parameters for the Pb(II) ion. The number of distances used in deriving the parameters is also listed. The O.x atom type corresponds to an oxygen bound to any atom. Distances are in Å, force constants are in kcal mol^{-1} Å^{-2}.

Atom	# of Distances	K_b	d_0
N.2	126	45	2.40
N.3	268	51	2.53
N.ar	360	44	2.60
O.x	1747	8	2.62

Table Vb. Statistical bond angle parameters for the Pb(II) ion. The number of angles used in deriving the parameters is also listed. Angles are in °, force constants are in kcal mol^{-1} rad^{-2}.

Set	# 1	# 2	# 3	# of Angles	K_θ	θ_0
	O.co2	Pb	O.co2	85	90.8	50.5
I	O.2	Pb	O.2	42	187.3	47.3
	N.ar	Pb	N.ar	128	98.3	63.8
	O.co2	Pb	O.co2	371	3.5	78.4
	O.2	Pb	O.2	364	2.1	76.6
II	N.ar	Pb	N.ar	380	19.7	80.2
	O.2	Pb	N.ar	185	23.1	79.5
	C.ar	N.ar	Pb	606	102.8	121.2
III	C.2	O.co2	Pb	191	22.9	96.8
	C.2	O.co2	Pb	171	28.9	120.5

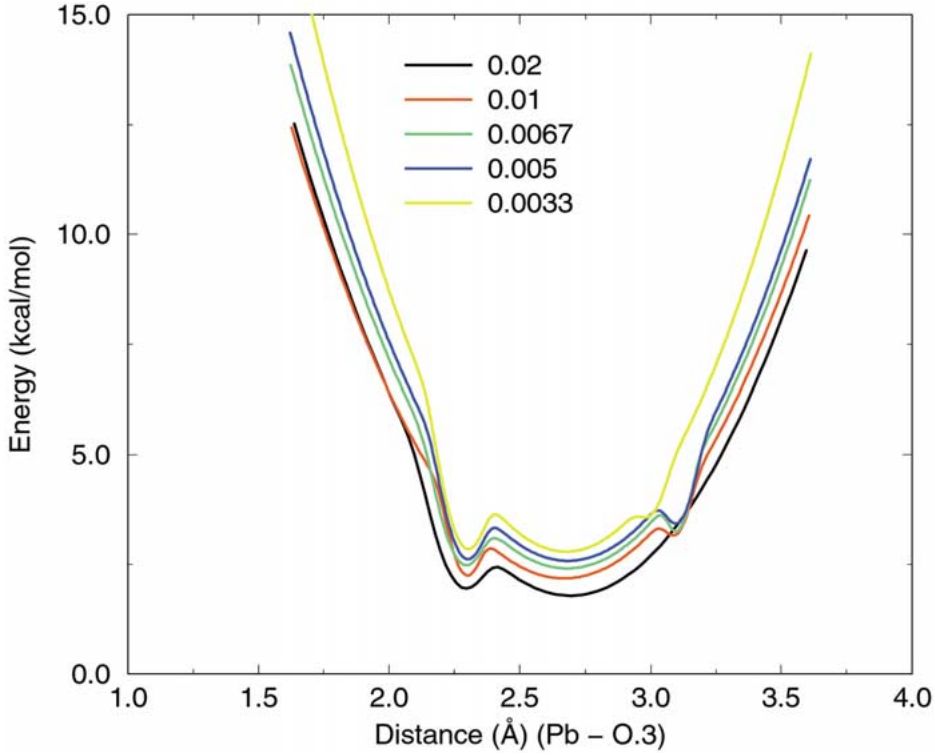

Figure 4. Bond potential energy for Pb(II)-O.3 as a function of distance. The curves are calculated using the different values of the binning-step listed in the figure. All distances are in Å.

Vb, respectively. For the nitrogens, the bond force constants have values of about 50 kcal mol^{-1} $Å^{-2}$ with equilibrium distances that vary from 2.4 to 2.6 Å. We found it difficult to calculate bond parameters for each oxygen type, due to the nature of the distributions, and so we calculated a single set of parameters for all oxygens (atom type O.x). We obtained an equilibrium distance of about 2.6 Å and, not unexpectedly, a very small force constant.

The bond-angle distributions involving a Pb(II) ion as the central atom are of complex character as they often contain more than one peak (see Figure 3(b) for examples). For many angles there are broad angle distributions at values larger than about 1.8 radians but we decided not to calculate bond angle parameters in these cases and instead treated these interactions using non-bonding interactions alone. The bond-angle parameters that we did calculate can be divided into sets I and II (Table Vb). Set I contains angles with equilibrium angles of between about 50° and 60° and large force constants. These correspond to cases where, for example, there are carboxylate or nitrate groups coordinating the Pb(II) and in which the fixed distance between the coordinating atoms results in a thin angle distribution. Set II has much lower force constants and equilibrium angles of about 80°. It is interesting to compare our parameters with those of Munro et al. who modeled metalloporphyrins (Munro et al., 1992). They used θ_0 equal to 60° and K_θ equal to 7.2 kcal mol^{-1} rad^{-2} for NPH–Pb(II)–NPH and θ_0 equal to 180° and K_θ equal to 40.3 kcal mol^{-1} rad^{-2} for NR2–M–NR2 with M being Fe(II) or Pb(II). The magnitudes of the force constants are in agreement with our results although the equilibrium angle, in the first case, is smaller than ours. Parameters for some angles involving Pb(II) as the terminal atom are also listed in Table Vb (set III). In the case of the angle C.2–O.co2–Pb, the two different sets of parameters were obtained by fitting to the two distinct peaks of the angle distribution shown in Figure 3(b).

To parametrize the alternative energy form, described in section 2.2, we use the bond and bond-angle distributions of Figures 3(a) and 3(b). The distributions are fitted to sums of three gaussians (see equation 8) so that the differences in the PMFs (equation 7) are minimized. The optimized parameters are shown in Tables VIa and VIb for the bonds and bond angles, respectively.

Table VIa. Coordination bond parameters for the NPE energy term. a_i is dimensionless, b_i is in kcal mol^{-1} and c_i is in Å.

Atom Bound to Pb(II)	a_1	b_1	c_1	a_2	b_2	c_2	a_3	b_3	c_3
N.2	0.0773	258.2	2.36	0.0489	436.4	2.49	0.0665	163.1	2.67
N.3	0.0067	780.2	2.36	0.0474	753.2	2.46	0.0102	630.9	2.60
N.ar	0.0349	133.8	2.52	0.0196	160.5	2.65	0.0030	604.6	2.79
O.2	0.0338	639.9	2.31	0.0328	29.5	2.61	0.0386	936.9	2.90
O.3	0.0030	655.6	2.30	0.0319	126.1	2.43	0.0268	383.8	2.70
O.co2	0.0161	562.6	2.23	0.0090	241.0	2.56	0.0101	72.3	2.71

Table VIb. Coordination bond angle parameters for the NPE energy term. a_i is dimensionless, b_i is in kcal mol^{-1} and c_i is in degrees. * For C.3-O.3-Pb, we employed the parameters of C.2-O.co2-Pb as this angle was not in the training set. **These parameters should be used when both oxygens are attached to the same atom like a nitro or a carboxy group otherwise the parameters described in the previous line should be taken.

	Angle		a_1	b_1	c_1	a_2	b_2	c_2	a_3	b_3	c_3
C.ar	N.ar	Pb	0.0423	275.8	72.2	0.0442	237.7	120.9	0.0010	828.0	131.8
C.3	N.3	Pb	0.0384	42.0	110.6	0.0407	231.8	123.8	0.0013	976.1	133.5
C.2	O.2	Pb	0.0223	707.5	100.3	0.0163	736.3	123.2	0.0051	318.7	132.4
C.2	O.co2	Pb	0.0291	674.5	96.8	0.0412	515.8	122.6	0.0433	945.6	160.4
*C.3	O.3	Pb	0.0291	674.5	96.8	0.0412	515.8	122.6	0.0433	945.6	160.4
N.2	O.2	Pb	0.0095	182.6	92.5	0.1503	96.0	99.6	0.0056	40.1	115.1
N.3	Pb	N.3	0.1046	61.69	75.6	0.0076	599.8	100.2	0.0331	130.3	137.5
N	Pb	N	0.0099	409.4	64.2	0.0305	103.9	79.6	0.0062	493.2	132.9
N	Pb	N.3	0.0388	290.5	67.0	0.0335	415.2	87.1	0.0020	272.6	123.2
N	Pb	O.3	0.0435	941.3	69.3	0.0471	992.1	106.0	0.0027	787.6	120.3
O.3	Pb	N.3	0.0602	53.1	67.6	0.0096	364.2	87.0	0.0243	11.8	128.9
O	Pb	N.3	0.0082	629.0	65.9	0.0254	568.6	74.5	0.0374	307.0	108.9
O.3	Pb	O.3	0.0334	995.7	61.9	0.0079	338.8	76.8	0.0312	620.4	127.8
O.3	Pb	O	0.0409	201.4	76.8	0.0166	618.3	114.6	0.0201	707.0	126.6
O	Pb	N	0.0250	409.8	51.0	0.0287	652.4	76.8	0.0442	482.3	120.9
O	Pb	O	0.0532	50.1	75.6	0.0185	20.1	131.1	0.0026	196.9	149.0
**O	Pb	O	0.0442	280.2	48.1	0.0210	210.0	76.2	0.0445	305.5	130.1

The step that we use to bin the data for the determination of the NPE energy-term parameters does have some effect on the results but the value of the step depends upon the number of data points and their range of values. For oxygen distances we used a step of 1/150 Å whereas for nitrogens we used 1/33 Å. For the angle calculations we used a 2° step for every case. The effect of the step size on the energy function is shown in Figure 4, where the bond energy is computed for the bond Pb–O.3 using functions determined using different binning-steps. The differences are relatively slight although larger binning-steps produce smoother curves, as expected. In general, it can be shown that the energy variation between two curves obtained with binning-steps, δ_1 and δ_2, is approximately equal to $-\beta \ln(\delta_1/\delta_2)$. Figure 5 shows the bond-angle energies for the C.co2-PB(II)-C.co2 bond angle determined using the NPE energy term (thin line) and from harmonic potentials (dashed and dotted lines) determined with the 'CSD' PMF method. It is clear that the NPE energy terms permit greater flexibility as they allow jumps between different energy wells whereas simulations of angles with a harmonic potential are constrained to remain in a single well.

Four different parameter sets for the Pb(II) ion were refined using the procedure described in section 2.3. These were, (1) the set 'CSD' PMF using the NPE energy term, (2) the set with the 'CSD' PMF harmonic

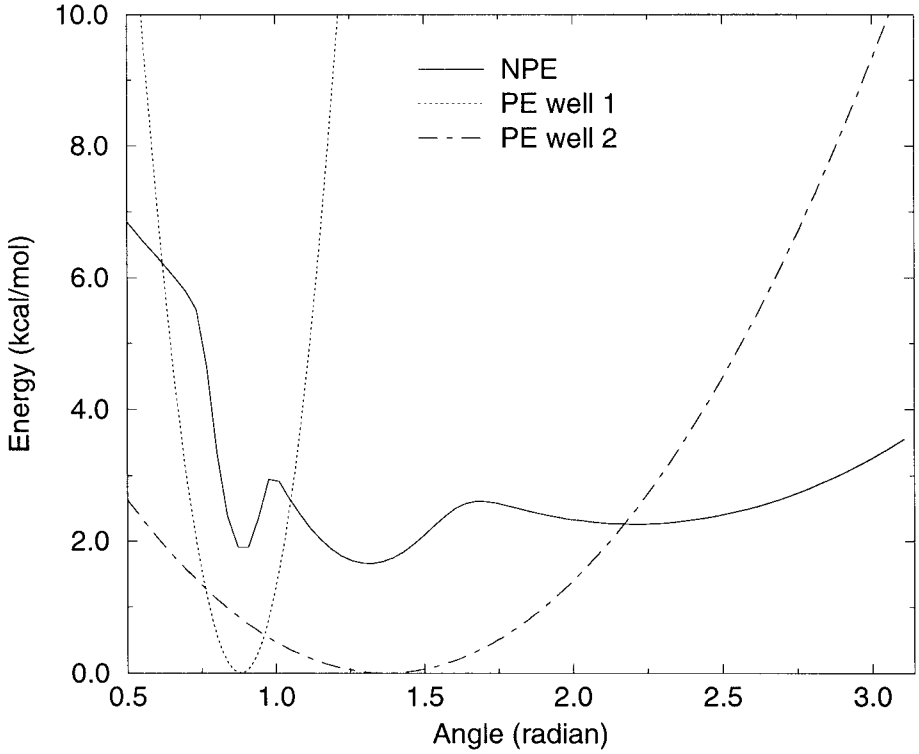

Figure 5. Energy function for the angle O.co2-Pb-O.co2. The dotted and dot-dashed lines are the 'CSD' PMF harmonic energy terms (see Table V) and the solid line is for the NPE energy term.

energy term and the sets (3) 'LJ1' and (4) 'LJ2' that contain only non-bonding (electrostatic and LJ) interactions between the Pb(II) ion and its neighbors. In sets (1), (2) and (3) the only two LJ parameters that were optimized were those defining the LJ radius and well-depth of the Pb(II) ion. In contrast, in set (4), the LJ parameters for the following 10 different types of LJ interaction were optimized separately: Pb–O.2, Pb–O.3, Pb–O.co2, Pb–N.2, Pb–N.ar, Pb–N.3, Pb–C.2, Pb–C.ar, Pb–C.3 and Pb–H. The optimizations with sets (1), (2) and (3) were started off with LJ parameters for the Pb(II) ion of $\epsilon = -0.2$ kcal mol^{-1}, $\sigma = 2.02$ Å. The final optimized values for the (ϵ, σ) pair were: (1) (−0.266,1.92) for the optimization with the NPE energy term; (2) (−0.349,1.84) for the optimization with the harmonic energy term and (3) (−0.452,1.73) for the 'LJ1' optimization. For the 'LJ2' set, we tried various optimization approaches including optimizing the ϵ_{ij} and σ_{ij} values or the A_{ij} and B_{ij} values for each interaction type in the following equation:

$$E(\text{vdW})_{ij} = 4\epsilon_{ij}\left[(\sigma_{ij}/r_{ij})^{12} - (\sigma_{ij}/r_{ij})^{6}\right] = A_{ij}/r_{ij}^{12} - B_{ij}/r_{ij}^{6}, \quad (9)$$

Table VII. Lennard-Jones parameters A_{ij} and B_{ij} optimized for the 'LJ2' model. Units are kcal mol^{-1} Å^{12} and kcal mol^{-1} Å^{6}, respectively.

Atom Bound to Pb(II)	A_{ij}	B_{ij}
O.2	1036214.75	7894.62
O.co2	3040112.00	2883.28
O.3	3029399.25	5068.26
N.ar	931939.81	4964.56
N.2	1898660.25	660.90
N.3	1721507.00	8177.21
C.ar	3418302.75	7137.35
C.2	3878556.50	1937.11
C.3	1170044.13	5202.91
H	3644106.50	1085.30

In the end, we found convergence faster and the results were more satisfactory when we optimized the A_{ij} and B_{ij} pairs. The final optimized values are given in Table VII.

The RMS coordinate deviations (RMSCD) between the structures (from the training set) obtained

Table VIIIa. RMSCDs between the energy minimized structures of the training set using the 'CSD' PMF NPE, the 'CSD' PMF harmonic, the 'LJ1' and 'the 'LJ2' models (see the text for a full description). The reference structures are the *ab initio* optimized ones. Best results are indicated in bold and the number of parameters required for each structure are listed in brackets after the RMSCDs. Units are in Å.

Optimization	Molecule			
	HABCES	PYCXPB	NONYAQ	RIMHAW
NPE	**0.5** (38)	**0.3** (62)	**0.5** (50)	**0.5** (20)
Harmonic	1.0 (14)	0.7 (22)	0.8 (18)	0.6 (8)
'LJ1'	0.7 (2)	1.0 (2)	0.6 (2)	2.1 (2)
'LJ2'	**0.5** (16)	**0.3** (12)	0.7 (16)	1.1 (8)

Table VIIIb. RMSCDs between the energy minimized structures using the 'CSD' PMF NPE, the 'LJ1' and the 'LJ2' models. The reference structures are the *ab initio* optimized ones. Best results are indicated in bold and the number of parameters required for each structure are listed in brackets after the RMSCDs. Units are in Å.

Optimization	Molecule						
	ZZZGZS	FICSIT	FILDIN	PASBAM	PBPHCY01	ROFKIG	KUJCOH
NPE	**0.7** (44)	**0.4** (44)	**0.3** (38)	1.0 (20)	0.5 (20)	0.8 (20)	0.9 (62)
'LJ1'	1.2 (2)	0.7 (2)	**0.3** (2)	**0.9** (2)	**0.2** (2)	**0.6** (2)	**0.3** (2)
'LJ2'	1.0(8)	0.5 (12)	0.6 (10)	1.2 (10)	**0.2** (6)	1.1 (12)	0.6 (14)
	RAQJAU	RASRIM	DAGHUO	GIMPUN	JUCCEP	GEXYOX	DOTTAH
NPE	**0.4** (20)	**0.9** (20)	**0.5** (20)	0.6 (56)	0.5 (38)	0.7 (20)	0.6 (74)
'LJ1'	1.2 (2)	1.5 (2)	0.6 (2)	**0.4** (2)	**0.2** (2)	0.8 (2)	**0.4** (2)
'LJ2'	**0.4** (10)	1.3 (12)	0.6 (10)	0.9 (12)	0.5 (10)	**0.2** (6)	1.3 (12)
	GIWQIM	TAZDPB	PRPHPB	FUYPAQ	WAVJOS	RAQMAX	
NPE	0.4 (20)	**0.2** (20)	**0.1** (20)	**0.3** (20)	**0.8** (56)	**0.4** (50)	
'LJ1'	0.8 (2)	*	0.2 (2)	0.6 (2)	1.5 (2)	1.5 (2)	
'LJ2'	**0.2** (8)	0.3 (6)	0.2 (8)	0.6 (6)	1.5 (12)	1.5 (10)	

*Energy minimization diverges.

after energy minimization (20000 maximum steps when no convergence attained) with various parameters sets and the *ab initio*-optimized structures are shown in Table VIIIa. These structures were the ones used in the training set. NPE gives better results with RMSCDs between 0.3 and 0.5 Å but the results obtained for the first two structures with the 'LJ2' model are comparable. The overall RMSCDs obtained by combining all 4 molecules (210 atoms in total) were 0.37, 0.62, 0.67 and 0.47 Å for the NPE, the harmonic, the 'LJ1' and the 'LJ2' models, respectively. To further compare these models, minimizations on a further set of twenty molecules were performed and are presented in Table VIIIb. These molecules, extracted from the CSD, were ZZZGZS (Conant, 1964), FICSIT(Lyukhin et al., 1998), FILDIN (Krasnova et al., 1987), PASBAM (Chandler et al., 1992), PBPHCY01 (Iyechika et al., 1982), ROFKIG (Uzoukwu et al., 1996), KUJCOH (Byriel et al., 1992), RAQJAU (Harrowfield et al., 1996), RASRIM (Skrzypczak-Jankun et al., 1997), DAGHUO (Alcock et al., 1984), GIMPUN (Mann et al., 1998), JUCCEP (Rogers et al., 1992), GEXYOX (Miyamae et al., 1988), DOTTAH (Esteban et al., 2000), GIWQIM (Hedinger et al., 1999), TAZDPB (Alcock et al., 1979), PRPHPB (Barkigia et al., 1980), FUYPAQ (Kepert et al., 2000), WAVJOS (Kokozei et al., 1992) and RAQMAX (Bytheway et al., 1996) (images of these molecules are not shown but are available upon request). Over the 24 molecules (4 in the training set and 20 in the test set) 15 molecules present have the smallest RMSCD with NPE, 8 with 'LJ1' and 6 with 'LJ2'. The RMSCDs for the NPE model go from 0.1 to 1.0 Å, for the 'LJ1' model from 0.1 to 2.1 Å (and for TAZDPB, the minimization fails) and for the 'LJ2' model from 0.2 to 1.5 Å. The mean RMSCD for the NPE model

is equal to 0.47 Å, to 0.80 Å for the 'LJ1' model (without TAZDPB) and 0.72 Å for the 'LJ2' model. The highest RMSCD obtained with NPE was with the molecule PASBAM. This molecule contains many 1–4 non-bonding interactions between atoms of type O.2 and O.3 and the Pb(II) ion. This interaction is not represented at all in the training set which may, in part, explain the larger RMSCD value. Equally, it would be interesting to integrate the 7 molecules with an RMSCD larger than 1 Å for the 'LJ2' model into the training set to see if the overall results could be improved.

To finish, we note that the number of parameters required for the NPE model is higher than for the other models. Thus, the NPE model needs between 20 and 74 parameters to describe the molecules in the training and test sets, the harmonic model between 8 and 18, the 'LJ1' model 2 and the 'LJ2' model between 6 and 16. It was our experience, however, that optimization of the NPE parameters was very robust as the optimization converged quickly and straightforwardly. In contrast, the optimization of the LJ parameters in the model 'LJ2' was much less well-behaved as it was difficult to constrain the parameters to have physically reasonable values. Thus the optimizations took longer even though fewer parameters were involved.

Conclusions

We have described a simple method to compute bond and bond-angle parameters for metals if sufficient experimental data is available to construct bond and bond-angle distributions. The method has been applied to a selection of Fe(II)-porphyrin and simple Cu(II) complexes and gives bond and bond-angle parameters that agree reasonably with those from other force fields. The computation of Pb(II) parameters is more complicated, mainly due to the less well-defined covalent character of the bond between this ion and the atoms that are coordinated to it and the fact that there are fewer structures from which to generate parameters. Nonetheless a set of parameters was refined based on the structures available in the CSD and, in addition, a MM energy term of novel form was proposed with the aim of better representing the multiple conformations displayed by Pb(II) in its complexes. The results we obtain are encouraging, although by no means definitive. Indeed, more atom types need to be included in the training set to test this approach on a broader range of molecules. Current work is aimed at refining our methodology further and at employing the parameter sets for molecular dynamics simulations of the leadzyme in explicit and implicit models of solvent.

Acknowledgements

The authors would like to thank Professor Michael Gilson who provided us with access to the Cambridge Structural Database at CARB/NIST and the referees for helpful comments. PA and MJF also acknowledge the Institut de Biologie Structurale – Jean-Pierre Ebel, the Commissariat à l'Energie Atomique and the Centre National de la Recherche Scientifique for support of this work.

References

Alcock, N.W., Curzon, E.H. and Moore, P. J. Chem. Soc., Dalton Trans. (1984) 2813.
Alcock, N.W., Herron, N. and Moore, P. J. Chem. Soc., Dalton Trans. (1979) 1486.
Allen, F.H., Davies, J.E., Galloy, J.J., Johnson, O., Kennard, O., Macrae, C.F., Mitchell, E.M., Mitchell, G.F., Smith, J.M. and Watson, D.G. J. Chem. Inf. Comput. Sci. 31 (1991) 187.
Allinger, N.L. J. Am. Chem. Soc. 99 (1977) 8127.
Barkigia, K.M., Fajer, J., Adler, A.D. and Williams, G.J.B. Inorg. Chem. 19 (1980) 2057.
Bernhardt, P.V. and Comba, P. Inorg. Chem. 32 (1992) 2638.
Bernstein, F.C., Koetzle, T.F., Williams, T.F., Meyer Jr. G.J.B., Brice, M.D., Rodgers, J.R., Kennard, O., Shimanouchi, T. and Tasumi, M. J. Mol. Biol. 112 (1977) 535.
Beveridge, K.A. and Bushnell, G.W. Can. J. Chem. 57 (1979) 2498.
Bol, J.E., Buning, C., Comba, P., Reedijk, J. and Strohle, M. J. Comput. Chem. 19 (1998) 512.
Brooks, B.R., Bruccoleri, R.E., Olafson, B.D., States, D.J., Swaminathan, S. and Karplus, M. J. Comput. Chem. 4 (1983) 187.
Byriel, K., Dunster, K.R., Gahan, L.R., Kennard, C.H.L., Latten, J.L., Swann, I.L. and Duckworth, P.A. Polyhedron 11 (1992) 1205.
Byrn, M.P. and Strouse, C.E. J. Am. Chem. Soc. 113 (1991) 2501.
Bytheway, I., Engelhardt, L.M., Harrowfield, J.M., Kepert, D.L., Miyamae, H., Patrick, J.M., Kelton, B.W.S., Soudi, A.A. and White, A.H. Aust. J. Chem. 49 (1996) 1099.
Chandler, C.D., Hampden-Smith, M.J. and Duesler, E.N. Inorg. Chem. 31 (1992) 4891.
Comba, P., Hambley, T.W. and Strohle, M. Helv. Chim. Acta 78 (1995) 2042.
Conant J. Inorg. Nucl. Chem. 26 (1964) 895.
Coord. Chem. Rev. 2001, 212, 1–168. Review articles on force field development for metal coordination complexes.
Cornell, W.D., Cieplak, P. and Kollman, P.A. J. Am. Chem. Soc. 118 (1996) 2309.
David, L., Lambert, D., Gendron, P. and Major, F. Leadzyme, in Ribonucleases, Methods in Enzymology, Nicholson, Alan W. (editor); Academic Press Inc., NY, 341 (2001) 518.
David, L., Luo, R. and Gilson, M.K. J. Comput. Chem. 21 (2000) 295.

Davis, M.E., Madura, J.D., Luty, B.A. and McCammon, J.A. Comp. Phys. Comm. 62 (1991) 187.
Derreumaux, P., Zhang, G., Schlick, T. and Brooks, B. J. Comput. Chem. 15 (1994) 532.
Dorsey, R. and Mayer, W.J. advances in Artificial Intelligence in Economics, Finance and Management Vol 1 (1994) 69.
Esteban, D., Banobre, D., de Blas, A., Rodriguez-Blas, T., Bastida, R., Macias, A., Rodriguez, A., Fenton, D.E., Adams, H. and Mahia, J. Eur. J. Inorg. Chem. (2000) 1445.
Foloppe, N. and Mackerell, A. J. Comp. Chem. 21 (2000) 86.
Hancock, R.D. Prog. Inorg. Chem. 37 (1989) 187.
Harrison, P.G. Coord. Chem. Rev. 20 (1976) 1.
Harrowfield, J.M., Miyamae, H., Shand, T.M., Skelton, B.W., Soudi, A.A. and White, A.H. Aust. J. Chem. 49 (1996) 1051.
Hay, B.P. Coord. Chem. Rev. 126 (1993) 177.
Hedinger, R., Kradolfer, T., Hegetschweiler, K., Worle, M. and Dahmen, K.-H. Chem. Vap. Deposition 5 (1999) 29.
Hoogstraten, C.G., Legault, P. and Pardi, A. J. Mol. Biol. 284 (1998) 337.
Hunger, J. and Huttner, G. J. Comput. Chem. 20 (1998) 455.
Hunger, J., Beyreuther, S., Huttner, G., Allinger, K., Radelof, U. and Zsolnai, L. Eur. J. Inorg. Chem. 6 (1998) 693.
Inoue, M.B., Fernando, Q., Villegas, C.A., Inoue, M. Acta Crystallogr., Sect.C (Cr. Str. Comm.) 49 (1993) 875.
Iyechika, Y., Yakushi, K., Ikemoto, I. and Kuroda, H. Acta Crystallogr., Sect. B 38 (1982) 766.
Jaguar 4.0, Schrödinger Inc., Portland, Oregon, 2000.
Kepert, D.L., Patrick, J.M., Skelton, B.W. and White, A.H. Aust. J. Chem. 41 (1988) 157.
Kokozei, V.N., Polyakov, V.R., Simonov, Yu.A. and Sinkevich, A.V. Zh. Neorg. Khim. 37 (1992) 1810.
Krasnova, N.I., Simonov, Yu.A., Korshunov, M.B. and Yakshin, V.V. Kristallografiya 32 (1987) 499.
Krisyuk, V.V., Baidina, I.A., Gromilov, S.A., Alekseev, V.I. and Prokhorova, S.A. Zh. Strukt. Khim. 38 (1997) 527.
Lyukhin, A.B.I, Poznyak, A.L., Sergienko, V.S. and Stopolyanskaya, L.V. Kristallografiya 43 (1998) 812.
Mackerell Jr., A.D., Bashford, D., Bellott, M., Dunbrack Jr., R.L., Evanseck, J.D., Field, M.J., Fischer, S., Gao, J., Guo, H., Ha, S., Joseph-McCarthy, D., Kuchnir, L., Kuczera, K., Lau, F.T.K., Mattos, C., Michnick, S., Ngo, T., Nguyen, D.T., Prodhom, B., Reiher III, W.E., Roux, B., Schlenkrich, M., Smith, J.C., Stote, R., Straub, J.E., Watanabe, M., Wiorkiewicz-Kuczera, J., Yin, D. and Karplus, M. J. Phys. Chem. B 102 (1998) 3586.
Mann, K.L.V., Jeffery, J.C., McCleverty, J.A. and Ward, M.D. J. Chem. Soc., Dalton Trans. 18 (1998) 3029.
Miyamae, H., Yoshinari, K., Hihara, G. and Nagata, M. Acta Crystallogr., Sect.C (Cr. Str. Comm.) 44 (1988) 1528.
Munro, O.Q., Bradley, J.C., Hancock, R.D., Marques, H.M., Marsicano, F. and Wade, P.W. J. Am. Chem. Soc. 114 (1992) 7218.
Press, W.H., Teukolsky, S.A., Vetterling, W.T. and Flannery, B.P. Numerical Recipes in Fortran 77, Cambridge University Press, 1996.
Qiu, D., Shenkin, P.S., Hollinger, F.P. and Clark Still, W. J. Phys. Chem. A 16 (1997) 3005.
Quanta, Molecular Simulation Inc., Waltham, MA.
Rogers R.D. and Bond, A.H. Inorg. Chim. Acta 192 (1992) 163.
Roux, B. and Karplus, M. J. Comp. Chem. 16 (1995) 690.
Sippl, M.J., Ortner, M., Jaritz, M., Lackner, P. and Flockner, H. Folding and design 1 (1986) 289.
Skrzypczak-Jankun, E. and Smith, D.A. Acta Crystallogr. section C 53 (1997) 579.
Uzoukwu, B.A., Adiukwu, P.U., Al-Juaid, S.S., Hitchcock, P.B. and Smith, J.D. Inorg. Chim. Acta 250 (1996) 173.
Winter, M. http://www.webelements.com
Woods R.J., Khalil, M., Pell, W., Moffat, S.H. and Smith Jr., V.H. J. Comp. Chem. 11 (1990) 297.
Zhihui, Z., Xinahe, B., Zhiang, Z. and Rongtia, C. J. Inorg. Chem. 13 (1997) 58.
Zimmer, M. Chem. Rev. 95 (1995) 2629.